AD-A118 685 DEFENCE RESEARCH ESTABLISHMENT ATLANTIC DARTMOUTH (NO--ETC F/G 20/1
PROPELLER CAVITATION NOISE INVESTIGATIONS IN A FREE-FIELD ENVIR--ETC(U)
JUN 82 L J LEGGAT

UNCLASSIFIED DREA-TM-82/E NL

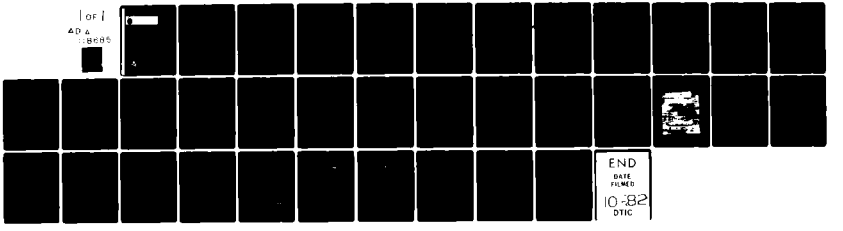

(3)

DEFENCE RESEARCH ESTABLISHMENT
ATLANTIC

# PROPELLER CAVITATION NOISE INVESTIGATIONS IN A FREE-FIELD ENVIRONMENT





D. R. E. A. TECHNICAL MEMORANDUM 82/E

RESEARCH AND DEVELOPMENT BRANCH
DEPARTMENT OF NATIONAL DEFENCE
CANADA

DEFENCE RESEARCH ESTABLISHMENT
ATLANTIC
DARTMOUTH N.S.

D R E A TECHNICAL MEMORANDUM 82/E

# PROPELLER CAVITATION NOISE INVESTIGATIONS IN A FREE-FIELD ENVIRONMENT

L. J. Leggat

June 1982

Approved by T. Garrett Director / Technology Division

DISTRIBUTION APPROVED BY

CHIEF D. R. E. A.

RESEARCH AND DEVELOPMENT BRANCH
DEPARTMENT OF NATIONAL DEFENCE
CANADA

## ABSTRACT

Cavitation is the dominant source of noise for cavitating propellers. It is generally agreed that the growth and collapse of cavitation bubbles creates a monopole acoustic source mechanism, which radiates sound in an omnidirectional pattern from the oscillating bubble. Hydrodynamic flows about propellers produce other types of cavitation besides bubble cavitation. Vortex cavitation occurs in the concentrated tip and hub vortices, and sheet cavitation can occur at the propeller blade leading edge. Each of these types of cavitation may have different acoustic source strengths and source spectra.

A propeller drive apparatus has been built at the Acoustics Barge at the Defence Research Establishment Atlantic. The fully instrumented barge is located in Bedford Basin, a large soft-bottom salt-water body of water near Halifax. A stationary propeller drive pod and near and far-field hydrophones are fixed to and suspended from the barge. Propellers designed to produce various types of cavitation have been tested in this facility.

Techniques have been developed to determine relationships between the far-field sound and the hydro-acoustic source mechanisms in the near-field of the propeller. Through cross-correlation a causality relationship is established which renders information about the spatial distribution of acoustic source strength on and near the cavitating propeller.

This paper describes this cavitation noise facility, reviews the theory and practice behind the measurement technique, and presents some results from tests with three different propellers. These tests included cavitation observations, far-field radiated noise and directivity measurements, and acoustic source localization.

## RÉSUMÉ

La cavitation est la principale source de bruit pour les hélices cavitantes. On concède en général que la formation et l'écrasement des bulles de cavitation constituent une source de bruit dont le rayonnement est omnidirectionnel depuis la bulle oscillante. Les écoulements des liquides autour des hélices produisent d'autres types de cavitation que celle des bulles. La cavitation de tourbillon se produit dans les tourbillons concentrés des pointes et des arbres, et la cavitation à poche peut se produire sur l'arête d'entrée de la pale. Chacun de ces types de cavitation peut avoir des puissances et des spectres acoustiques divers.

Un mécanisme d'entraînement des héices a été construit à la Péniche de recherches acoustiques au Centre de recherches pour la défense Atlantique. Cette péniche remplie d'instruments, est située dans le bassin de Bedford, une grande masse d'eau salée à fond mou près de Halifax. Une nacelle d'entraînement d'hélice stationnaire et des hydrophones de champ proche et de champ éloigné sont fixés à la péniche ou suspendus d'elle. Des hélices conçues pour produire divers types de cavitation ont été essayées dans cette installation.

On a mis au point des techniques permettant de déterminer les rapports entre le son dans le champ éloigné et les mécanismes de la source hydro-acoustique dans le champ proche de l'hélice. Au moyen de doubles corrélations, on a dégagé un rapport de cause à effet qui fournit des informations sur la distribution spatiale de la puissance de la source acoustique sur l'hélice cavitante et près d'elle.

La présente communication décrit cette installation d'étude du bruit de cavitation, examine la théorie et la pratique de la technique de mesure et présente des résultats d'essais portant sur trois hélices différentes. Ces essais comprenaient des observations sur la cavitation, des mesures du bruit émis dans le champ éloigné et de la directivité, et la localisation de la source acoustique.

TABLE OF CONTENTS

## NOTATION

| | |
|---|---|
| $a_o$ | speed of sound |
| $f_i, \underline{f}$ | local surface stress tensor, vector |
| $p$ | far field acoustic pressure or local pressure |
| $\nabla p_n$ | normal pressure gradient |
| $r_o$ | distance between source and far field measuring point |
| $S$ | surface |
| $T_{ij}$ | effective stress tensor |
| $t$ | time |
| $\hat{t}$ | retarded time $\hat{t} = t - \frac{x}{a_o}$ |
| $u$ | velocity |
| $u_{i,j}$ | velocity vector |
| $u_n$ | normal velocity |
| $V$ | volume |
| $X$ | Dimensionless propeller radius |
| $x$ | $x = (x-y)$ distance from source point to far field microphone |
| $x_i, \underline{x}$ | space co-ordinate to indicate point of sound detection in the far field |
| $y_i, \underline{y}$ | space co-ordinate used in source region |
| $\delta_{ij}$ | *Kronecker* delta tensor |
| $\lambda$ | wavelength of sound |
| $\rho$ | ambient density |
| $\rho'$ | density fluctuation |
| $\tau$ | retarded time delay between two realizations of fluctuating variables |
| $\tau_{ij}$ | viscous stress tensor |
| $\dot{}$ | a dot over a symbol indicates derivatives with respect to time. |

## 1. INTRODUCTION

The noise produced by hydrodynamic flow past rotating propellers has been a subject of considerable speculation and controversy. It is generally agreed that the growth and collapse of cavitation is the major source of noise from a cavitating propeller. However propeller cavitation appears in many forms, and is routinely found in the low pressure regions produced by the flow around a propeller. Sheet, bubble, tip vortex, hub vortex, and cloud cavitation are familiar terms in propeller hydrodynamics. Design methods can allow the designer to discriminate against a noisy form of cavitation in favour of quieter types in order to achieve an overall improvement in the propeller noise level. However, the choice of which type of cavitation to avoid is not always clear.

It is entirely probable that each type of cavitation possesses a unique source strength and spectrum. Further, the noise produced by the types of cavitation may vary quite differently with changes in cavitation number, propeller advance coefficient, and Reynolds number.

Early research into propeller cavitation noise was carried out by Ross and McCormick[1], using a stationary "eggbeater" apparatus. The noise data they collected were found to agree well with a simplified theory developed from dimensional arguments. They also confirmed that the noise was omnidirectional and that the intensity was inversly proportional to the square of the distance and the square of the frequency.

Much of the work in propeller cavitation noise which took place after these experiments was not published in the open literature, however a review of propeller cavitation noise by Strasberg[2] has provided a very clear account of the state of propeller cavitation noise research during the 25 years leading up to 1977. In the paper he discusses problems associated with measuring and scaling noise from propellers operating in towing tanks and water tunnels. He concludes that, given the required amount of care to closely model the physical environment, it could be feasible to make full scale noise predictions from model experiments for tip vortex cavitation noise.

Work in cavitation noise from model propellers has been in progress at the Netherlands Ship Model Basin, Depressurized Towing Tank[3] for some time now. Results reported in 1974[4] showed that measurements of the noise from a ship's propeller could be correlated with the propeller cavitation state, thus allowing quantitative comparisons on a model scale. A later paper[5] addressed the problem at hand: the relative impact of various types of cavitation on the propeller cavitation noise. Three propellers were tested, which produced back sheet, back bubble, and tip vortex cavitation. Comparative measurements

in the depressurized towing tank showed that back bubble cavitation is an extremely loud form of cavitation. Noise from tip vortex and back sheet cavitation were found to be almost equal. However, because of the presence of back sheet cavitation on the tip vortex propeller, this comparison was not absolute. Later, Swedish[6] and Russian[7] work confirmed the relative source strengths as bubble cavitation strongest, followed by face sheet, back sheet, and tip vortex, for light to moderately loaded propellers.

The degree of success that has been achieved in correlating model with full scale noise data has not been reported in the open literature, however at least one reference to model test work in a depressurized towing tank indicates that acceptable scaling of the model noise data is possible[8].

Given an environment which is correctly scaled and has low background noise levels, it appears within the state-of-the-art to predict full scale noise levels from model test data. However, no facilities are capable of producing a completely scaled measuring environment. Thus the ability to scale the noise over all frequencies and for a wide range of operating conditions becomes a subject of some difficulty and much interest.

An understanding of the factors influencing the acoustic source strength and spectrum of propeller cavitation, and of how the various types of cavitation scale can be furthered through investigating the basic hydrodynamic acoustic mechanisms which produce the noise. Some interesting work in this regard was reported recently by Latorre.[9] From noise measurements and observations of a tip vortex producing propeller operating in a water tunnel, he developed the concept of an envelope for tip vortex cavitation inception noise. The envelope corresponded to the range of cavitation numbers between the cavitation number where there was noise and no visible tip vortex and that where the tip vortex was visible and attached to the tip of the propeller. In this envelope the noise from the vortex was characterized by many bursts or spikes in the signal, produced by the expansion of small bubbles or nuclei entering low pressure regions of the vortex core. This nuclei expansion was used as the basis for an analytic method which modelled the flow field, cavitation nuclei and tip vortex, and calculated the noise resulting from the bubble expansion. Calculated and measured tip vortex cavitation noise envelopes showed very good agreement. Once verified in this manner, this model can be used for analytic parametric investigations and for scaling tip vortex inception noise results from model to full scale. The key to the success of this work was determining the fundamental phenomena and mechanisms responsible for the cavitation noise.

Currently, propeller cavitation noise mechanisms are studied using two methods. The first, propeller viewing and sound ranging, is carried out in full scale ships. The propellers are viewed through ports in the bottom of the ship's hull, above the propeller. Ideally, the viewing and sound ranging are performed simultaneously. Determining the spectral content of the first type of cavitation to occur on the blade is fairly simple. Generally, tip vortex cavitation appears first. However, once more than one form occurs, it is impossible to discriminate the contribution to the far-field signal from the various forms of cavitation on the blade.

The second method used to study propeller cavitation noise is through model testing in water tunnels and depressurized towing tanks. Unless special propellers are built, this procedure suffers from the same deficiencies as the full scale experiments. It offers a more controlled hydrodynamic test environment, but is complicated by problems associated with performing sound measurements inside the tunnel or tank. The resulting sound data represent the near-field propeller pressure in a highly reverberant and noisy environment. It is therefore extremely difficult to obtain meaningful acoustic data, and virtually impossible to determine the source strengths of the different forms of cavitation.

This paper describes a facility and method for obtaining the acoustic source strength of propeller cavitation using model propellers in a free-field environment. The method, based on Curle's formulation of flow noise theory,[10] makes use of the cross-correlation between the normal pressure gradient in the near-field of the source, and the far-field acoustic pressure. The technique follows from established methods for determining acoustic source strengths in aerodynamic flows about solid surfaces,[11,12] in air jets,[13] and on surfaces of fan blades.[14]. The method discriminates in favour of the near-field pressure gradient fluctuations that contribute to the far-field acoustic pressure. Because the pressure gradient is directly proportional to the normal velocity of the cavitation volume, through Euler's equation, a direct evaluation of the local acoustic source strength, intensity, spectrum, and correlation area is possible. A spatial plot of these parameters can be developed by moving the near-field pressure gradient hydrophone about in the vicinity of the propeller and its wake. Using this method, the different forms of cavitation can be studied, leading to more accurate scaling laws and prediction techniques

Initial experiments with this facility have concerned the measurement of noise from three propellers which produce a variety of types of cavitation including tip vortex, hub vortex, and back bubble. The cavitation state on the propeller was observed while the far-field noise and its directivity were measured. The local acoustic source strength distribution was measured for one propeller which produced tip and hub vortex cavitation.

This paper will address the problem of performing propeller cavitation noise experiments in a free-field environment. The experimental facility and its special features will be described. A discussion will follow of the analytic methods developed to allow source investigations. Special instrumentation and propellers designed for particular experiments will be described. The paper will conclude with some typical results of tests with cavitating propellers.

## 2. FACILITY AND FEATURES

The propeller cavitation noise tests took place in Bedford Basin, a large body of salt water located between Dartmouth and Halifax as shown in Figure 1. The Basin has a mean depth of 50m, and the bottom is covered by a deep layer of silt, giving it good acoustic absorption properties. It is free of significant amounts of shipping. Thus the ambient noise levels are low, especially during the winter months when a thin layer of surface ice prevents noise from wind and waves. Because of the good underwater acoustic properties of this area, it was chosen for the site of an acoustic calibration facility, the DREA Acoustic Barge. In recent years, modifications to the barge have allowed propeller cavitation noise tests to be carried out in the Basin.

### 2.1 DREA Acoustic Barge

The DREA Acoustics Barge is a moored floating steel structure measuring 36m long and 17m wide.[15] It contains a large well, 18m by 9m, open to the sea. The working area around the well is covered by a large deckhouse which encloses the laboratory, machinery rooms, and support facilities. To ensure low noise levels, power is supplied to the barge by a submarine cable. A 35 kVA diesel generator provides auxiliary power.

Drawings of the barge are shown in Figure 2. The well, shown in Figure 2B, is spanned just above the waterline by two moveable catwalks, supported on rails attached to each side of the well. Each catwalk is equipped with a travelling trolley, which supports a light support station capable of handling up to 130 kg of equipment. Equipment or hydrophones suspended from the trolleys can be placed accurately in the well at depths varying from 2.4m to 27.0m. The rotation of the station shafts is controlled from the laboratory and is coupled to analysis and plotting equipment for calibration of hydrophones and projectors.

The barge facility is also equipped with a heavy mounting station, capable of handling loads up to 2700 kg. It can be suspended from mounting brackets located at either end of the well. Heavy equipment is handled with an overhead crane rated at 4500 kg. The crane allows loads to be placed anywhere inside the deckhouse, and is essential for setting up the variety of experiments which take place at the barge.

## 2.2 Propeller Drive Assembly

The arrangement for driving model propellers consists of a propulsion pod suspended below the barge from the heavy station as shown in Figure 3. The pod, whose centreline is at a depth of 2.6m, can be rotated through 180 degrees. A variable speed D.C. electric torpedo motor with a rated power of 26.5 kW is installed in the pod, and drives model propellers with a diameter typically of 250mm, up to a maximum revolution rate of 2000 rpm. The drive assembly is fitted to allow measurement of propeller rpm, torque and power. The motor is cooled using liquid carbon dioxide fed from cannisters in the barge.

## 2.3 Special Instrumentation

The experiments for which this facility was designed require a large number and variety of hydrodynamic and acoustic measurements. Because the analysis technique requires pressure gradient measurements, a special purpose hydrophone was built. The depth of the propeller posed special problems for visualization of the propeller and its cavitation state. Finally, the propellers themselves had to be designed for the bollard condition in which they were to operate.

### 2.3.1 Pressure Gradient Hydrophone

Pressure gradient is difficult to measure directly and so it is usually approximated using a pressure difference technique. The two hydrophones that form the pressure difference pair must be phase and gain matched, and mounted in such a way that they do not interfere with one another acoustically. Further, if the pressure gradient is to be measured in a regime of fluid flow such as a propeller wake, the hydrophone must be designed to give a true measure of the static pressure fluctuation.

The hydrophone designed and built at DREA[16] is shown in Figure 4. It consists of two ceramic cylinders mounted to a pitot-static tube type probe. The two ceramic elements can be gain and phase matched during calibration by adding capacitance as required to one of the elements. The spacing between the two elements (38.0mm) makes the hydrophone effective over the frequency range of 1 to 20 kHz.

The calibration of the hydrophone was completed at DREA using the substitution technique. The response curve for the hydrophone, which is shown in Figure 5 for a frequency band of 1 to 10 kHz, has the expected positive slope of 6 dB per octave. This curve is for sound arriving from the end-fire direction. The directivities at 2 and 8 kHz are also shown in Figure 5. The dipole directivity produced by the opposite-phase pair of ceramics shows a broad-side rejection of 25 dB. This broad-side rejection varies from 10 dB at 1 kHz to 32 dB at 10 kHz. The reduction of broad-side rejection as frequency is reduced is consistent with the degradation of signal-to-noise ratio with increasing wavelength. When the wavelength is long compared to the element spacing, the difference in level between the two is small. The signal-to-noise ratio problem limits the effective response of the hydrophone at the low frequency end, and the finite distance between the ceramic elements limits the response at the high frequency end.

### 2.3.2 Flow Visualization

Because the propeller operates at a depth of 2.6m, direct observation of the cavitation state from the surface is not possible. An observation capability is provided by a periscope, which is mounted to one of the mobile catwalks on the barge. The propeller may be viewed from any angle by moving the catwalk and periscope mount. Lighting is provided by means of two high power strobe lamps mounted in water tight containers, and fixed to a frame above the drive pod. Photographs may be taken through the periscope using a standard camera back and adaptive lenses.

### 2.3.3 Propellers

The propellers used with the facility are two-bladed and 250mm in diameter. They are designed especially for the bollard pull condition. Experiments are proceeding with three propellers: one designed to produce hub and extreme tip vortex cavitation, a second to produce bubble cavitation, and a third of a more conventional design to produce hub and tip vortex cavitation. Drawings of the three propellers are shown in Figure 6. The propellers were designed using a lifting line method[17] and then analysed analytically using lifting surface techniques.[18]

The first propeller, referred to as tip vortex propeller no. 1, was designed with a circulation distribution biased heavily toward the propeller blade tip as shown in Figure 7. Such a distribution produces a strong tip vortex, and as a result, heavy cavitation in this region of the blade. The pitch, camber, and thickness for the blade sections were then chosen to avoid sheet and bubble forms of cavitation on the blade surfaces.

The second propeller, the back bubble propeller, was designed to produce back bubble cavitation only. Because tip vortex and hub cavitation are difficult to avoid, the main effect was directed toward thickening and applying camber to the blade sections so that back bubble cavitation would be produced. A more conventional circulation distribution was chosen (Figure 7). The tip and hub were unloaded so that vortex types of cavitation could be delayed.

The final propeller, tip vortex propeller no. 2, was given the same circulation distribution as the back bubble propeller, but the blade sections were pitched, thickened, and cambered in such a way as to avoid bubble and sheet types of cavitation. The results from this propeller can be compared with those from tip vortex propeller no. 1 to examine the effect of tip loading on the propeller cavitation state and noise.

Future plans call for the construction of a propeller designed to produce sheet cavitation from a circulation distribution identical to that of the tip vortex propeller no. 2 and back bubble propellers.

## 3. THEORETICAL DEVELOPMENT

Ideally, propeller noise studies should be carried out in an entirely anechoic environment. Under these circumstances multiple reflections would not confuse the data, and reverberation and background noise would not be a problem. However, at the Acoustics Barge, while reverberation and background noise are not a problem, reflection from the water surface and barge side walls can distort the radiated noise data, especially during directivity measurements.

### 3.1 Sound Propagation Model

A theoretical and experimental study was carried out to investigate the acoustic transmission anomaly produced by the surface and barge wall reflections. A computer program was written to determine the sound power spectrum of the acoustic energy received by a hydrophone of specified position under the barge, and within the confines of the well, from an omnidirectional source. Ray acoustics were assumed and acoustic paths with up to four barge wall and/or water surface reflections were considered significant. The contribution of the basin bottom was considered negligible because of the high absorptive coefficient of the medium.

For a given source and receiver position, the computer program determines which propagation paths are effective, the magnitude and phase of the pressure arrivals at the receiver for each propagation path, and the resultant sound power spectrum at the receiver. In determining the magnitude and phase of pressure arrivals, the program takes into consideration the water surface reflection and barge wall reflection where applicable. Because the barge wall has finite depth, a method for calculating the effects of diffraction is incorporated, and is based on the theory according to Pierce.[19]

The mathematical model was verified by an experiment which employed a projector with a flat frequency response as the source and an omnidirectional hydrophone as the receiver. A comparison of theory and experiment for one condition is shown in Figure 8. The sound propagation anomaly is plotted against frequency over the band 100 Hz to 10 kHz. The agreement between the two sets of results is within 4 dB, except at low frequencies near 100 Hz, where ray acoustics no longer apply, and at frequencies where phase cancellation occurs. Here the ambient noise in the basin limits the depth of the cancellation troughs.

The acoustic propagation anomaly can be determined experimentally and mathematically. Experience has shown that the experimental method is very time consuming, especially where measurements are made at a number of locations to determine propeller noise directivity patterns. The mathematical model is superior in these instances for correcting the noise data for the propagation anomaly.

## 3.2 The Causality Correlation Technique

The method of correcting far-field levels for the propagation anomaly in the previous section is suitable for comparing noise levels from various propellers, and for determining noise directivity. The diagnostic capability is limited to these two applications. Two point methods involving simultaneous near and far-field measurements offer additional diagnostic capabilities, and in some cases simplify the data acquisition and analysis process.

To extract the most benefit from two point methods, it is desirable to measure the variable in the near-field responsible for the sound generation. In the case of a loud speaker, for example, the crucial variable is the acceleration of the speaker cone. The acceleration of a vapour cavity wall must be measured in experiments with cavitating propellers. The difficulty involved in performing this measurement makes an alternate approach very attractive. In the near-field of the propeller, the vapour cavity accelerations are related to the pressure gradient through Euler's equation. By making this substitution, it is possible to arrive at a technique which determines the absolute source strength of the cavitation by cross-correlating the near-field pressure gradient and far-field acoustic pressure signals. The method has the added advantage that the cross-correlation record distinguishes the direct and reflected paths. The contribution from reflections can then be simply eliminated from the analysis procedure.

### 3.2.1 Application of Curle's General Fluid Dynamic Noise Equation

The acoustic radiation from a region of unsteady flow containing a surface is given by Curle's generalized solution to the Lighthill equation[10] [see Figure 9].

$$a_o^2 \rho'(\underline{x},t) = \int_S \left[\frac{\delta}{\delta t}(\rho u_n)\right] \frac{dS}{4\pi x} - \frac{\delta}{\delta x_i} \int_S \left[f_i + \rho u_i u_n\right] \frac{dS}{4\pi x}$$

$$- \frac{\delta^2}{\delta x_i \, \delta x_j} \int_V \left[\frac{T_{ij}}{4\pi x}\right] dV \qquad (1)$$

Where $\rho'$ is the incremantal density disturbance relative to the ambient density $\rho$, and $a_o$ the ambient speed of sound. The square brackets denote evaluation at retarded time $t = t - x/a_o$. The first two integrals are associated with noise generated between the flow and the surface S which may deform with a velocity $u_n$. The quantity $f_i$ represents the local stress acting at each point on the surface. The vector $\underline{f}$ may comprise both shear stress and normal stress components. The third integral is the Lighthill volume integral for turbulence-generated quadrupole noise where $T_{ij}$, the effective stress tensor is given by.

$$T_{ij} = \rho u_i u_j + \tau_{ij} + (p - a_o^2 \rho') \, \delta_{ij} \tag{2}$$

where $\rho u_i u_j$ is the Reynolds stress, $\tau_{ij}$ the viscous stress and $(p - a^2\rho') \, \delta_{ij}$ the thermal stress.

In the geometric and acoustic far-field; $r_o^2 >> S$, $r_o >> \lambda$; the spatial derivatives can be shown to become time derivatives and $r_o = (\underline{x} - \underline{y}) \approx x$ such that

$$p(\underline{x},t) \approx \frac{1}{4\pi x} \int_S \left[(\rho \dot{u}_n)\right] dS + \frac{x_i}{4\pi x^2 a_o} \int_S \left[\frac{\delta}{\delta t} (f_i + \rho u_i u_n)\right] dS + \frac{x_i \, x_j}{4\pi x^3 a_o} \int_V \left[\frac{\delta^2 T_{ij}}{\delta t^2}\right] dV \tag{3}$$

For hydrodynamic flow noise, the quadrupole noise is minimal, and so attention is directed to the two surface integrals. For cases where cavitation occurs on propeller blades and at low Mach numbers, the contributions from the second term are small giving

$$p(\underline{x},t) \approx \frac{1}{4\pi x} \int_S \rho \dot{u}_n \, (t - x/a_o) \, dS \tag{4}$$

The acoustic radiation results from monopoles close to the surface of the blade and in the wake associated with the growth and collapse of cavitation.

In the near-field, the normal velocity component is related to the normal pressure gradient by Euler's equation of linear momentum

$$\frac{\delta}{\delta t} \, u_n = - \frac{1}{\rho} \nabla p_n \tag{5}$$

where $\nabla p_n$ is the normal pressure gradient. Substituting equation (5) into equation (4) we obtain

$$p(\underline{x},t) \approx -\frac{1}{4\pi x} \int_S \nabla p_n \, (t - x/a_o) \, dS \tag{6}$$

3.2.2 The Causality Formalism

The development of the causality formalism follows Reference 11. If both sides of equation (6) are multiplied by the far-field radiated pressure at a new time, t', time averaging yields:

$$\overline{p(t) \, p(t')} \approx -\frac{1}{4\pi x} \int_S \overline{\nabla p_n \, (y,t) \, p(\underline{x},\hat{t}')} \, dS \tag{7}$$

If p and $\nabla p_n$ are stationary random variables

$$\overline{pp(\underline{x},\tau)} \approx \frac{1}{4\pi x} \int_S \overline{\nabla p_n \, p} \, (\tau + x/a_o) \, ds; \; \tau = t'-t \tag{8}$$

Then restricting our attention to the mean square acoustic pressure, $\tau = o$

$$\overline{p^2} \, (\underline{x}) = \frac{1}{4\pi x} \int_S \overline{\nabla p_n \, p(x/a_o)} \, dS \tag{9}$$

Thus the contribution to the mean square sound pressure at a far-field point $\underline{x}$ arriving from an element above the blade surface $dS(\underline{y})$ where $\nabla p_n$ is being measured is given by the integrand of equation (9). This quantity may be viewed as the strength of the acoustic source at that point, and for the case where the monopole sound radiation is dominant, as described earlier, will be called the monopole source strength. Differentiating equation (9), we obtain the expression for the acoustic source strength.

$$\overline{\frac{dp^2}{dS}} = \frac{1}{4\pi x} \overline{\nabla pp}(x/a_o) \tag{10}$$

Typically, the correlation function will be similar to that shown in Figure 10. The amplitude of the correlation function is evaluated at the appropriate time delay thus yielding a source strength associated with the monopole in the region of the measurement.

The magnitude and phase of the source region's pressure intensity spectrum may be evaluated simply by performing the Fourier transform of the cross-correlation function in the vicinity of the appropriate time delay $x/a_o$.

For propeller cavitation noise studies, the technique holds considerable potential. In situations where many forms of cavitation are present on a propeller, the near-field pressure gradient hydrophone can be traversed across the diameter of the propeller, and axially along the wake. By performing a cross-correlation between the far-field and pressure gradient hydrophones at each measurement point, the absolute acoustic source strengths, and distribution of strength for all types of cavitation can be determined.

## 4. TYPICAL RESULTS

The experiments with this facility have consisted of cavitation observation and photography, and far-field radiated noise measurements with the three experimental propellers. These tests have been conducted over the speed range of from 300 to 2100 rpm. Directivity measurements were carried out for each propeller. Also, one set of tests has been completed with the cross-correlation technique for acoustic source location. The pressure gradient hydrophone was traversed axially and parallel to the wake of tip vortex propeller No. 2. The cross-correlation between near and far-field transducers gave some indication of the region of noise generation from this propeller.

### 4.1 Cavitation Observations

Sketches of the cavitation observed on the three propellers are shown in Figure 11 for various revolution rates. These sketches were derived from photographs taken through the periscope.

For tip vortex propeller no. 1, the photographs show the gradual development of tip vortex cavitation with increasing rpm until the maximum revolution rate, where the tip and hub vortices are very strong and ropy. The back bubble propeller photographs show the development of tip vortex cavitation initially. This is followed by back bubble cavitation and a wash out of any tip vortex-type structure. The photographs for tip vortex propeller no. 2 show essentially the same sort of results as for tip vortex propeller no. 1, except that the tip vortex is not as strong.

### 4.2 Far-Field Radiated Noise

The radiated noise was measured in a frequency band of 0-5 kHz. Each propeller was tested over the range of revolution rate from 300 to 2100 rpm. Cavitation inception speeds were noted, and the noise was recorded for later analysis.

The results of these tests are shown in Figure 12. Here the source spectrum level in the 0-5 kHz band is plotted against propeller revolution rate. The inception of cavitation types is indicated by the arrows. The tip vortex propeller no. 1 produced the most noise in this band except at revolution rates below 1150 rpm where it was the quietest of the three propellers. This propeller shows a gradual increase in noise with the inception of tip and hub vortex cavitation. The most significant region of noise increase is between 1000 and 1800 rpm. The rms noise level at these rpm's showed large fluctuations (±5 dB) indicative of unstable flow or cavitation. Extended periods of observation, however, showed no spot cavitation or separated flow on the blade. At the highest rpms, the overall spectrum level actually decreased. The rms noise level in this rpm regime varied very little (less than 0.5 dB), indicating more stable conditions.

Tip vortex propeller no. 2 produced the same unstable conditions in the region of maximum rate of increase in the noise level. Fluctuations in the overall level of ±6 dB were typical. The conditions again became stable at the higher revolution rates. The source of the instability is not yet known. It has not been established whether the unstable region is associated with the cavitation at the propeller blade or with the vortex collapse in the propeller wake.

The noise from the back bubble propeller is the least intense in the moderate to high rpm range. This result contradicts the findings of other research into the relative intensity of various types of cavitation,[5,7] however, these propellers are operating in an extreme condition of high loading at a low advance coefficient. The tip and hub vortex cavitation formed under these conditions is considerably stronger than that which would be found with moderate to lightly loaded propellers.

Noise spectra for two revolution rates tested are shown in Figure 13 and 14. The influence of surface reflections is evident from the equally spaced humps and depressions in the spectra. Above 1 kHz, the spectrum level falls off at the rate of 6 dB per octave. Below this frequency, the spectra have a good deal of structure. The characteristics of the low frequency sound from the propellers will be a subject of future study.

### 4.3 Propeller Noise Directivity

The directional characteristics of the propeller radiated noise were measured by positioning the far-field hydrophone at various angles in the vertical plane containing the propeller axis. The directivity at 1 kHz and 1880 rpm for the three propellers is shown in Figure 15. The data shown in this figure have been corrected using the transmission anomaly computer program to eliminate the interference effect from surface and barge wall reflections. The tip vortex no. 2 and the back bubble propellers are omnidirection to within 1 dB over the angles tested. This pattern is typical of monopole types of sources such as cavitation. The directivity pattern of the tip vortex propeller No. 1 is omnidirectional to within 1 dB except at angles of 10 and 5 degrees where the level is 5 to 6 dB higher than at other angles. While it is not entirely clear at this time what causes this increase in the on-axis direction, it is thought that it might be caused by higher order source mechanisms such as dipoles. The dipole radiates in a figure eight pattern. If its axis were aligned with that of the propeller, it might cause increases in the noise in the on-axis direction.

### 4.4 Source Localization

A source localization scan of the trailing hub and tip vortices was carried out using tip vortex propeller No. 2 in order to determine the region from which tip vortex cavitation noise emanates. The pressure gradient hydrophone was positioned 290mm away from the blade tip in a plane perpendicular to the propeller axis and pointing at the axis. It was then traversed

axially from a position 0.25m upstream of the propeller to one 2.5m downstream. Cross-correlations between the near-field pressure gradient and the far-field acoustic pressure were computed at a number of points between these two extremities. Also the flow at each station was observed using the periscope. The hydrophone did not enter the wake at any time; it simply traversed along beside the vortex streets being shed by the propeller hub and blade tips.

Because the pressure gradient hydrophone becomes noisy below 1 kHz, the near and far-field signals were high-pass filtered at 1 kHz. They were low-pass filtered at 10 kHz, the maximum frequency of interest for these particular tests. The signals from the two hydrophones were amplified in two matched precision measuring amplifiers, and cross-correlated using a probability and a correlation function analyser.

A typical cross-correlation function derived from these tests is shown in Figure 16. The amplitude of the cross-correlation function $\overline{\nabla pp}$ is plotted against time delay. The first and most significant peak is produced by the direct path, and the time delay of the peak, $\tau$, = 17.4 ms. is equal to the amount of time required for sound to travel from the near to far-field hydrophone. The second peak is produced by the surface reflected path and arrives later because of the additional distance associated with this path. The monopole source strength is computed by evaluating the magnitude of the direct path peak in the correct units and substituting this value into equation (10) to arrive at the local monopole source strength, $\overline{dp^2}/dS$.

Results for the trailing vortex scan are shown in Figure 17. The top figure shows the pressure gradient as a function of distance along the wake, while the bottom figure shows the local monopole source strength. The pressure gradient, $\overline{\Delta p^2/\Delta x^2}$, remains relatively constant from a point 0.25m upstream of the propeller to the point where the tip vortices were observed to collapse. After this point, the pressure gradient drops off at a rate of the reciprocal of the distance squared.

The monopole source strength, $\overline{dp^2}/dS$, increases gradually from a point 0.25m behind the propeller. It shows no significant increase at the propeller plane, but continues to its maximum value at the point downstream of the propeller where the vortices were observed to collapse. While the resolution of this curve is coarse, it clearly indicated that the majority of sound produced by developed tip vortex cavitation comes from the region of vortex collapse and not from the region of vortex generation at the propeller blade tips. The resolution of these

measurements can be improved by moving the pressure gradient hydrophone closer to the wake. This was not attempted initially for fear of damaging either the propeller or hydrophone. As experience is gained with the use of the facility, higher resolution measurements will be performed.

## CONCLUSIONS

The Defence Research Establishment Atlantic's cavitation noise facility offers a potent facility for analysing radiated noise from propeller cavitation. The environment is well suited to acoustic studies. The Basin has low background noise levels, a stable temperature over the year, and a highly acoustically absorptive bottom.

The propeller drive assembly and specially designed model propellers produce various forms of cavitation typical of those found on full scale propellers. Although the operating conditions of the model propellers cannot be matched to full scale applications, it is not the intent to perform model studies with this facility. Rather it is designed to provide a capability for investigations into the hydro-acoustic mechanisms of propeller cavitation.

Results reported in this paper show that comparative noise measurements for various propellers, exhibiting different cavitation forms, can be performed over a wide frequency range. In addition, the cavitation state can be observed directly using a periscope, and propeller noise directivity can be measured using a correction for surface and barge wall reflections. The method of localizing accustic sources in the near-field of the propeller by using cross-correlation techniques indicates that the principle region of noise generation from tip vortices comes from the region of vortex collapse.

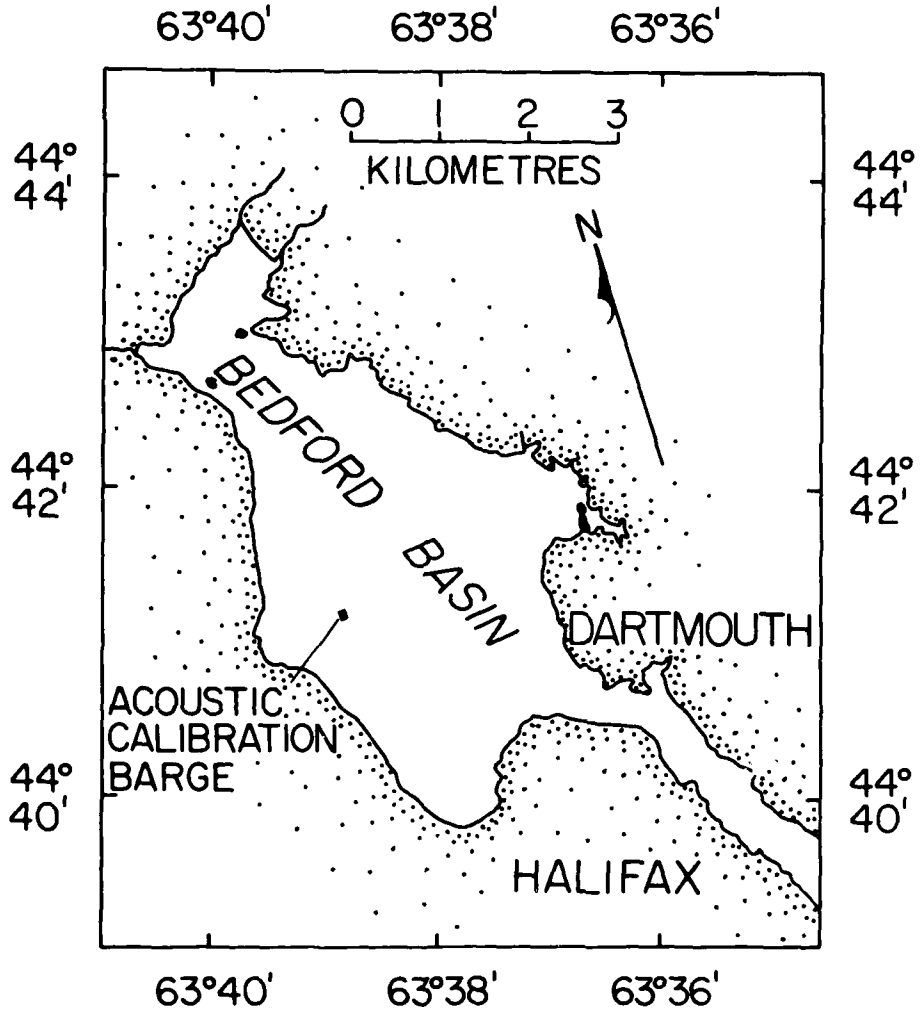


FIGURE 1. BEDFORD BASIN SHOWING LOCATION OF ACOUSTIC CALIBRATION BARGE

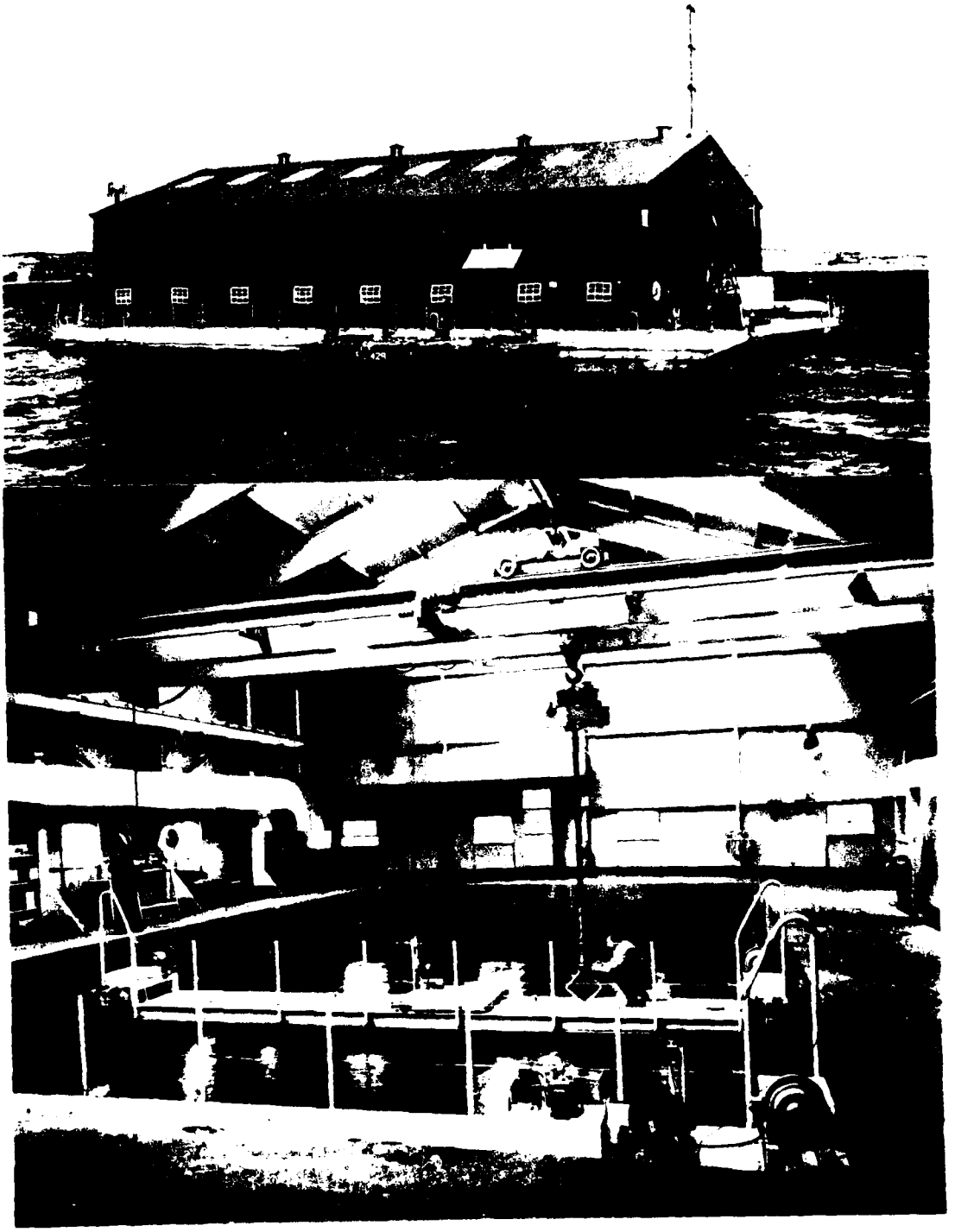

FIGURE 2. [illegible] OPERATIONS PLANT

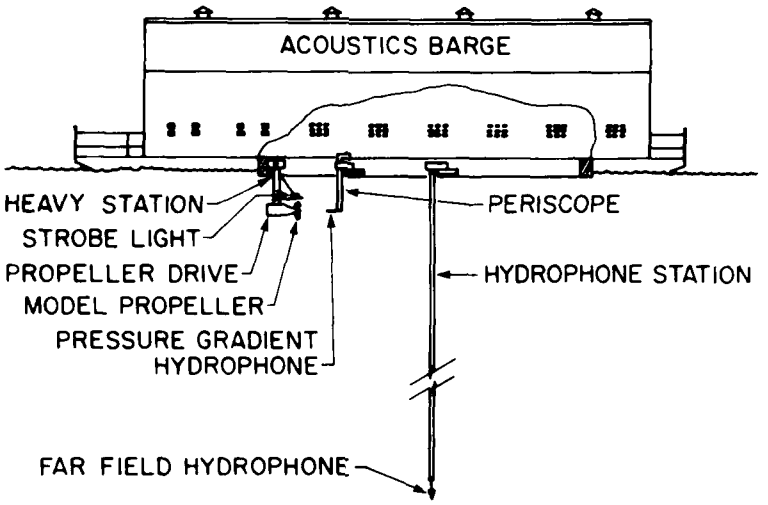


FIGURE 3. PROPELLER DRIVE AND HYDROPHONE LAYOUT

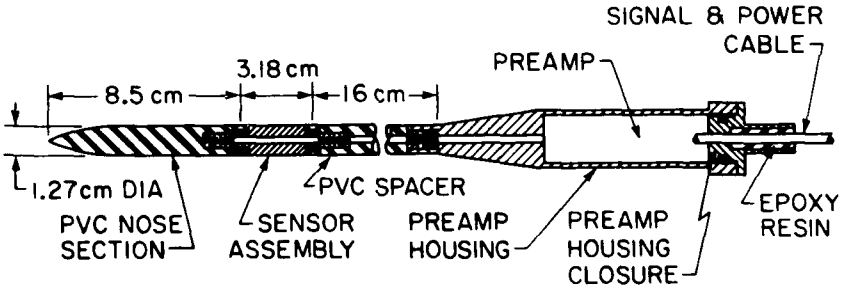


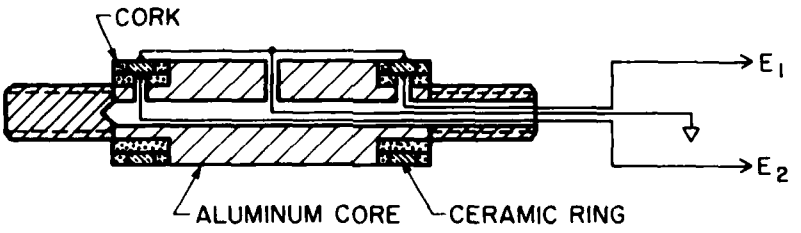


FIGURE 4. PRESSURE GRADIENT HYDROPHONE

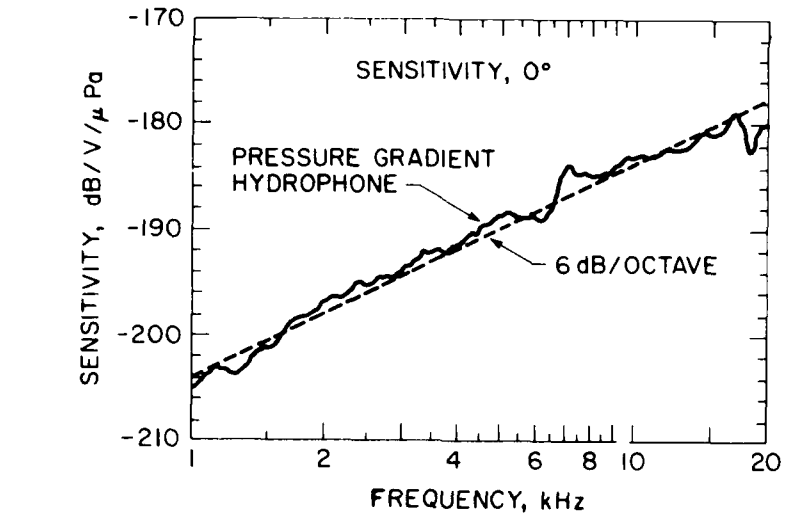


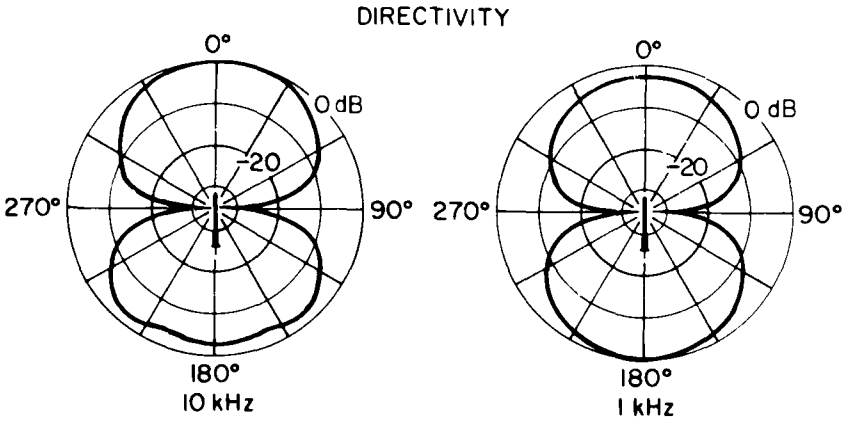


FIGURE 5. PRESSURE GRADIENT HYDROPHONE CALIBRATIONS

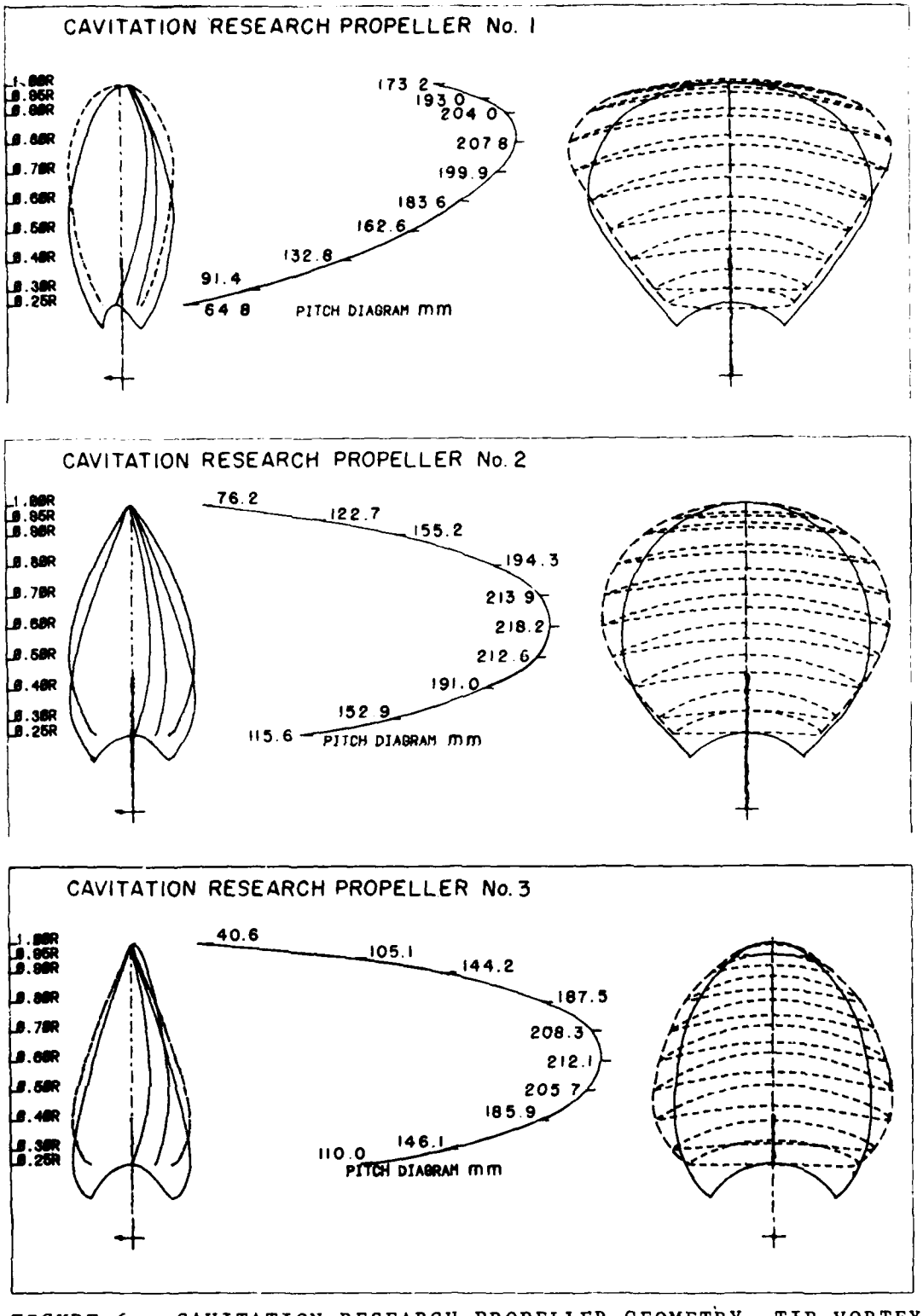


FIGURE 6. CAVITATION RESEARCH PROPELLER GEOMETRY, TIP VORTEX PROP. NO.1, TIP VORTEX PROP. NO.2, AND BACK BUBBLE PROP.

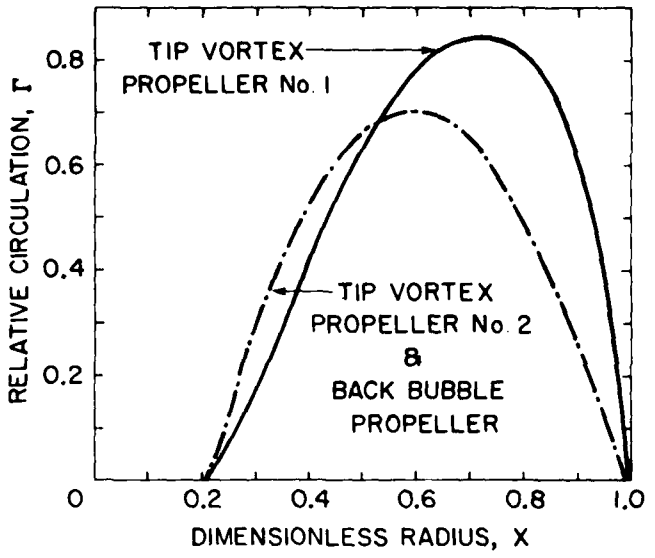


FIGURE 7. PROPELLER CIRCULATION DISTRIBUTIONS

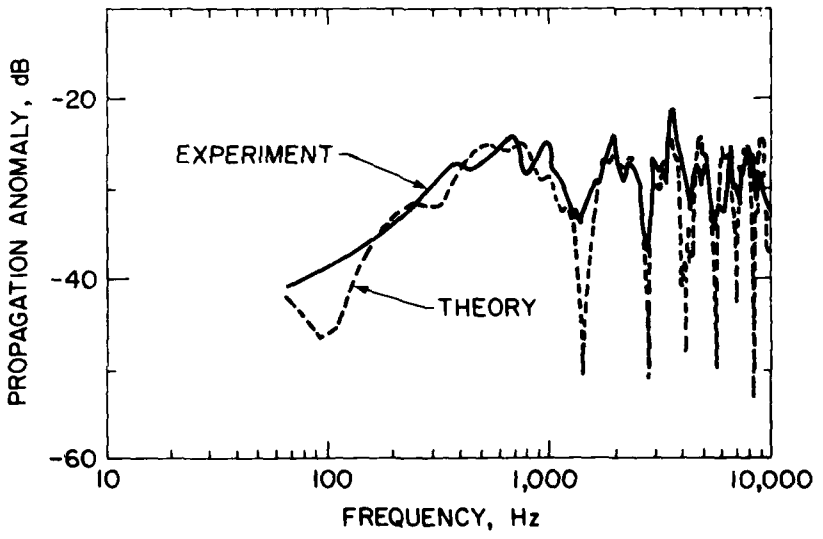


FIGURE 8. COMPARISON OF MEASURED AND CALCULATED PROPAGATION ANOMALIES

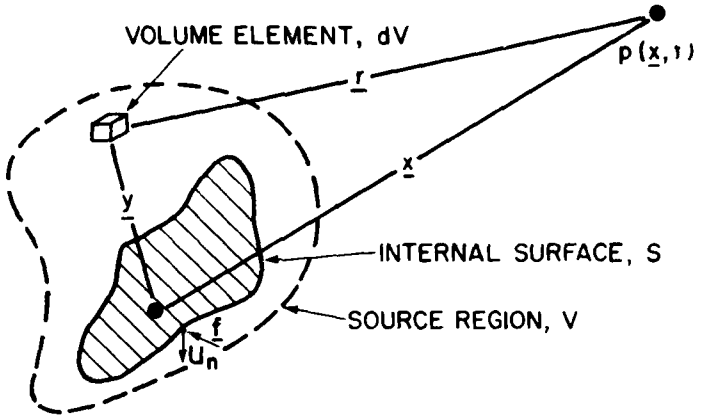


FIGURE 9. TERMINOLOGY FOR GENERALIZED NOISE SOURCE

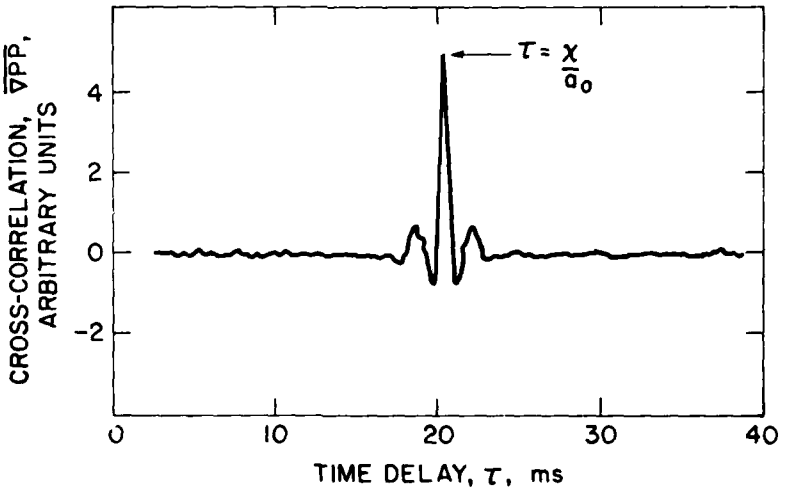


FIGURE 10. CROSS-CORRELATION FUNCTION

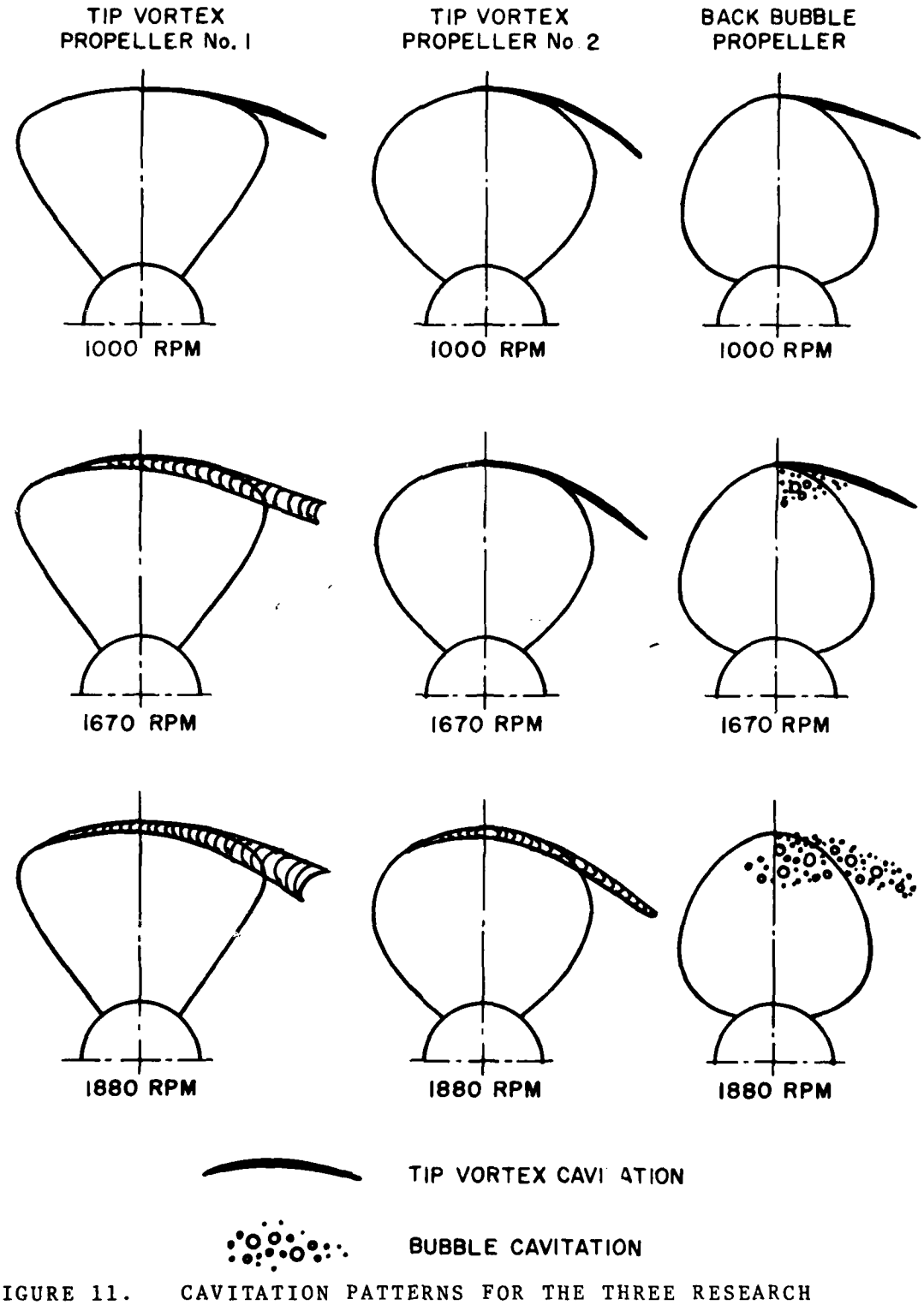


FIGURE 11. CAVITATION PATTERNS FOR THE THREE RESEARCH PROPELLERS

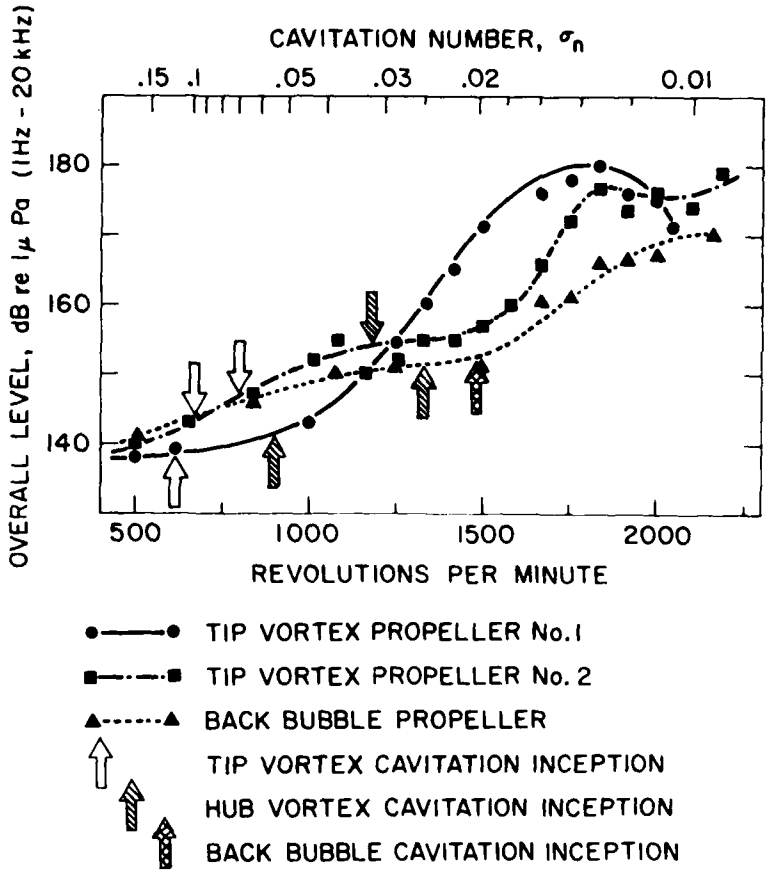


FIGURE 12. OVERALL NOISE LEVELS FOR THE THREE RESEARCH PROPELLERS

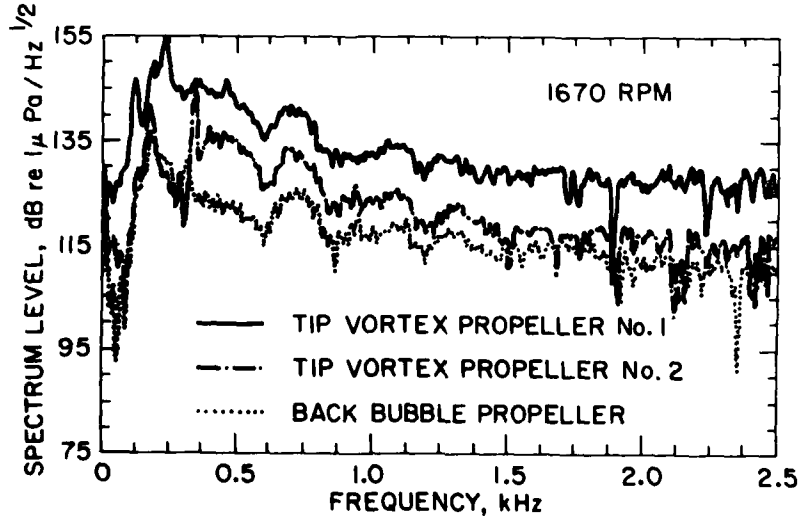


FIGURE 13. SPECTRUM LEVELS AT 1670 RPM

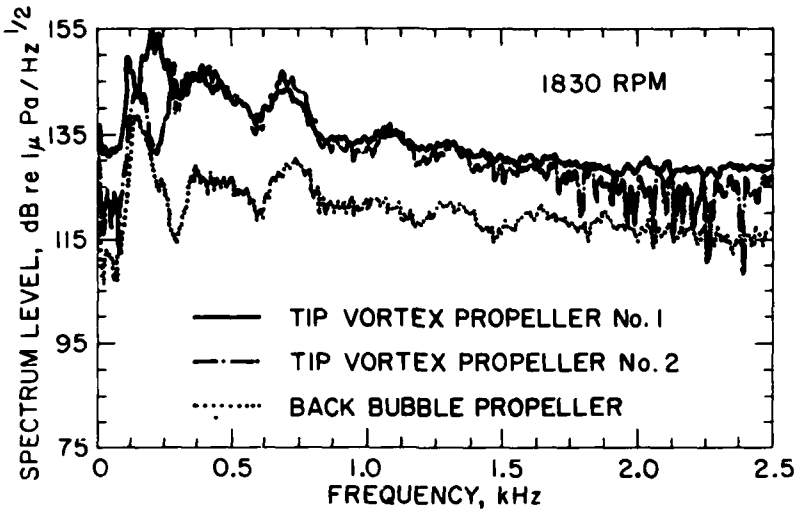


FIGURE 14. SPECTRUM LEVELS AT 1830 RPM

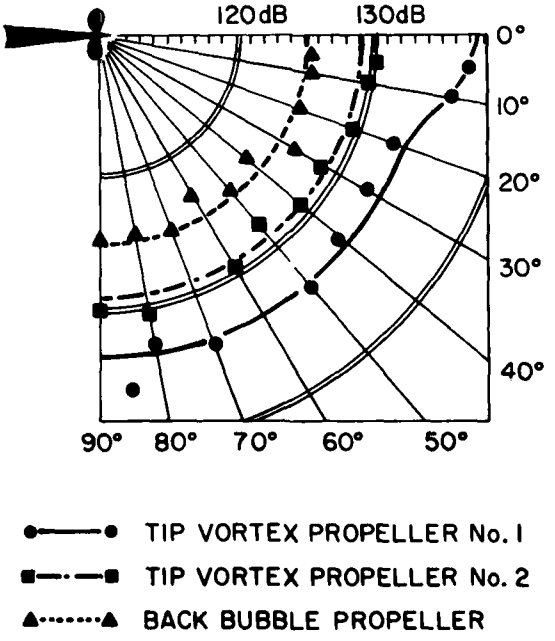


FIGURE 15. PROPELLER NOISE DIRECTIVITY AT 1kHz, 188 rpm

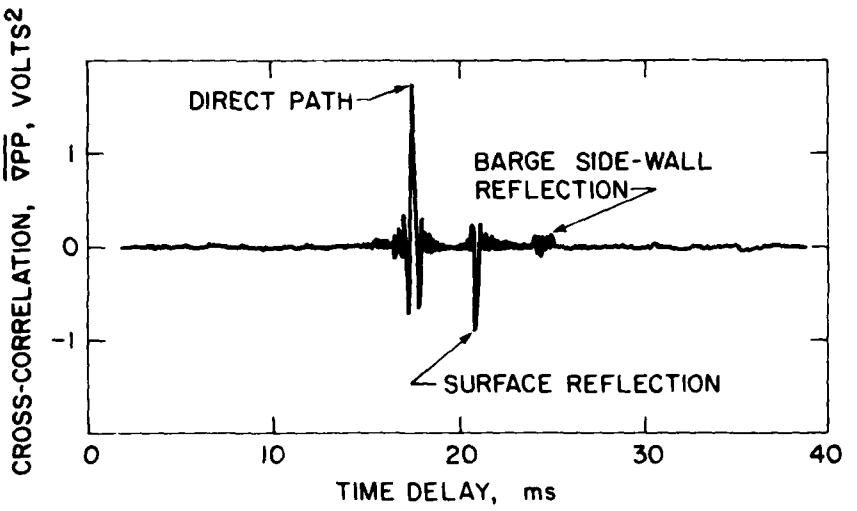


FIGURE 16. CROSS-CORRELATION OF NEAR-FIELD PRESSURE GRADIENT AND FAR-FIELD PRESSURE

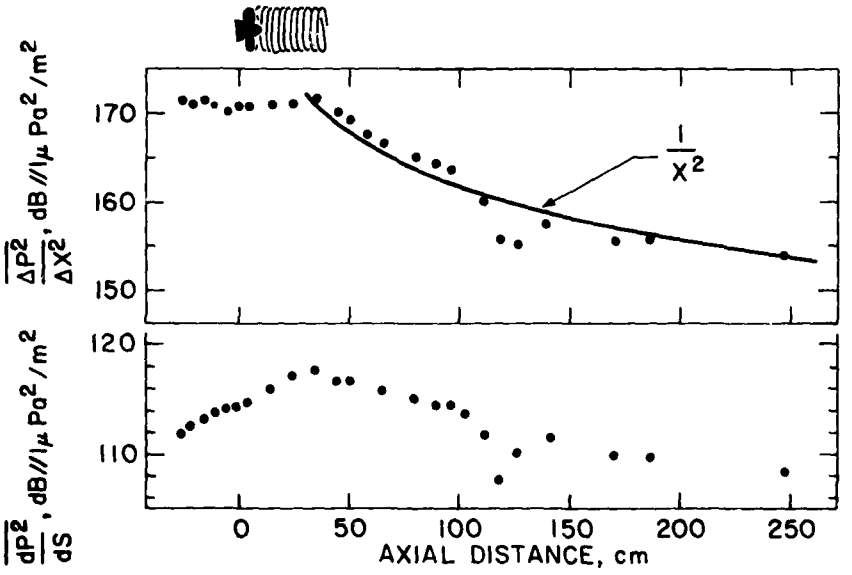


FIGURE 17. PRESSURE GRADIENT AND ACOUSTIC SOURCE STRENGTH AT POINTS PARALLEL TO THE PROPELLER AXIS

## REFERENCES


1. Ross, D. and McCormick B.W., Jr., "A Study of Blade Surface Cavitation Noise", Ord. Res. Lab. Rept. 7958-115, Oct, 1948

2. Strasberg, M., "Propeller Cavitation Noise After 25 Years of Study", ASME Noise and Fluids Engineering Symposium, Winter Annual Meeting, Atlanta Georgia, Dec, 1977.

3. Oosterveld, M.W.C., and van Oossanen, P., "Recent Tests in the NSMB Depressurized Towing Tank", SNAME First Ship Technology Research Symposium, Aug, 1975.

4. Stuurman, A.M., "Fundamental Aspects of the Effect of Cavitation on the Radiated Noise", Symposium on High Powered Propulsion of Large Ships, Part 2, Wageningen, The Netherlands, Dec, 1974.

5. Noordzij, L., van Oossanen, P., and Stuurman, A.M., "Radiated Noise of Cavitating Propellers", ASME Noise and Fluids Engineering Symposium, Winter Annual Meeting, Atlanta, Georgia, Dec, 1977.

6. Bark, G. and van Berlekom, W.B., "Experimental Investigations of Cavitation Noise", Twelfth Symposium, Naval Hydrodynamics, Washington, 1979.

7. Matveyev, G.A. and Gorshkoff, A.S., "Cavitation Noise Modelling at Ship Hydrodynamics Laboratory", Twelfth Symposium, Naval Hydrodynamics, Washington, 1979.

8. Leggat, L.J., Ligtelijn, J.Th. and Kennedy, J.L., "Propeller Design Studies for the Acoustic Research Ship CFAV QUEST", Nineteenth Meeting, ATTC, Ann Arbor, July 1980.

9. Latorre, R., "Propeller Tip Vortex Cavitation Noise Inception" SNAME, Propellers '81, Virginia Beach, May 1981.

10. Curle, N., "The Influence of Solid Boundaries on Aerodynamic Sound" Proc. Roy. Soc. (London) Ser. A231, 1955.

11. Siddon, T.E., "Surface Dipole Strength by Cross-Correlation Method", JASA, Vol. 53, No. 2, Feb, 1973.

12. Pan, Y.S., "Cross-Correlation Methods for Studying Near and Far Field Noise Characteristics of Several Flow-Surface Interaction Problems", Presented to the 87th meeting of the ASA, Apr, 1974.

13. Regan, D.R. and Meecham, W.C., "Multiple Turbojet Noise Suppression Studies Using Cross-Correlation Techniques", JASA, Vol. 63, No. 6, June 1978.

14. Leggat, L.J. and Siddon, T.E., "The Aeroacoustic Mechanism of Rotor-Vortex Interaction", JASA, Vol. 64, No. 4, Oct, 1978.

15. McMahon, G.W., "New Floating Laboratory Facilitates Underwater Acoustic Measurements", Canadian Electronics Engineering, Feb, 1961.

16. Fanning, B.L., "A Pressure Gradient Hydrophone for Propeller Noise Studies", DREA Informal Communication, Oct, 1981.

17. Manen, J.D. van, "Fundamentals of Ship Resistance and Propulsion Part B",. International Shipbuilding Progress, Vol. 4, No. 30, Feb 1957.

18. Taso, S.K.S., "Documentation of Programs for the Analysis of Performance and Spindle Torque of Controllable Pitch Propellers", MIT Dept. of Ocean Eng. Report 75-8.

19. Pierce, A.D., "Diffraction of Sound Around Corners and Over Barriers" JASA, Vol. 55, No. 5, May 1974.

Unclassified

Security Classification

**DOCUMENT CONTROL DATA - R & D**

(Security classification of title, body of abstract and indexing annotation must be entered when the overall document is classified)

| | |
|---|---|
| 1 ORIGINATING ACTIVITY<br>Defence Research Establishment Atlantic | 2a. DOCUMENT SECURITY CLASSIFICATION<br>Unclassified<br>2b. GROUP<br>Tech. Memo. |

3 DOCUMENT TITLE

PROPELLER CAVITATION NOISE INVESTIGATIONS IN A FREE-FIELD ENVIRONMENT

4 DESCRIPTIVE NOTES (Type of report and inclusive dates)

DREA TECHNICAL MEMORANDUM

5 AUTHOR(S) (Last name, first name, middle initial)

LEGGAT, L. JOHN

| 6 DOCUMENT DATE | 7a. TOTAL NO. OF PAGES | 7b. NO. OF REFS |
|---|---|---|
| JUNE 1981 | 36 | 19 |

| 8a. PROJECT OR GRANT NO. | 9a. ORIGINATOR'S DOCUMENT NUMBER(S) |
|---|---|
| | DREA TECH MEMO 82/E |
| 8b. CONTRACT NO. | 9b. OTHER DOCUMENT NO.(S) (Any other numbers that may be assigned this document) |

10 DISTRIBUTION STATEMENT

UNLIMITED

| 11. SUPPLEMENTARY NOTES | 12. SPONSORING ACTIVITY |
|---|---|
| | |

13. ABSTRACT


Cavitation is the dominant source of noise for cavitating propellers. It is generally agreed that the growth and collapse of cavitation bubbles creates a monopole acoustic source mechanism, which radiates sound in an omnidirectional pattern from the oscillating bubble. Hydrodynamic flows about propellers produce other types of cavitation besides bubble cavitation. Vortex cavitation occurs in the concentrated tip and hub vortices, and sheet cavitation can occur at the propeller blade leading edge. Each of these types of cavitation may have different acoustic source strengths and source spectra.

A propeller drive apparatus has been built at the Acoustics Barge at the Defence Research Establishment Atlantic. The fully instrumented barge is located in Bedford Basin, a large soft-bottom salt-water body of water near Halifax. A stationary propeller drive pod and near and far-field hydrophones are fixed to and suspended from the barge. Propellers designed to produce various types of cavitation have been tested in this facility.

Techniques have been developed to determine relationships between the far-field sound and the hydro-acoustic source mechanisms in the near-field of the propeller. Through cross-correlation a causality relationship is established which renders information about the spatial distribution of acoustic source strength on and near the cavitating propeller.

This paper describes this cavitation noise facility, reviews the theory and practice behind the measurement technique, and presents some results from tests with three different propellers. These tests included cavitation observations, far-field radiated noise and directivity measurements, and acoustic source localization.


DSIS
78-078


ATE
LME